World Research Journal of Applied Physics
ISSN: 0976-7673 & E-ISSN: 0976-7681, Vol. 1, Issue 1, 2010, pp-14-19.
Available online at http://www.bioinfo.in/contents.php?id=52

ELECTRICAL AND DIELECTRIC PROPERTIES OF ZIRCONIUM DOPED NICKEL-ZINC FERRITE

MAHINDRAKAR ROHINI, ALGUDE S.G. AND BIRAJDAR D.S.*
Department of Physics, S.C.S. College, Omerga, 413606, MS, India.

Abstract- Zirconium doped Nickel-Zinc ferrites of composition $Ni_{0.7+x}Zn_{0.3}Zr_xFe_{2-2x}O_4$ were prepared by standard double sintering ceramic technique. The single-phase cubic spinel structures of the samples were confirmed from X-ray diffraction patterns. Electrical properties namely DC-resistivity as a function of temperature were studied for ferrite samples. Dielectric properties such as dielectric constant (έ), dielectric loss (ε″) and loss tangent (tanδ) have been investigated at constant frequency with varying temperature.
Keywords- Ferrites, ceramic, electron hopping, d.c. electrical resistivity

Introduction

Ni-Zn ferrites are the most versatile electronic ceramic materials suited for high frequency application in the telecommunication field [1]. Ni-Zn ferrites show good magnetic properties for technical applications [2]. The interesting physical and chemical properties of ferrospinel depend upon the method of preparation [3], site preference of cations among the available tetrahedral (A) site and octahedral [B] site.

Nickel ferrite is an inverse spinel, where as Zinc ferrite is normal spinel. Hence it is interesting to study Ni-Zn ferrite. Ni-Zn ferrites are soft magnetic materials for high frequencies applications. These ferrites are used in radio frequency circuits, high quality filters, rod antennas, transformer core, read/write heads for high speed digital tape and operating devices [4]. The electric and dielectric properties are most important properties of ferrites, depending on the processing conditions, sintering temperature and time, chemical composition, the amount and type of additives [5]. The study of electrical resistivity produces valuable information on the behaviour of free and localized electric charge carried in the studied samples. In Ni-Zn ferrites, Zn^{2+} volatilization at high temperatures results in the formation of Fe^{2+}ions, there by increasing the electron hopping and reducing the resistivity [6,7]. The electrical resistivity of Ni-Zn ferrites processed through standard double sintering ceramic technique was studied as a function of temperature. The dielectric constant and dielectric loss were studied as the function of temperature.

Experimental

Ni-Zn ferrite of composition $Ni_{0.7+x}Zn_{0.3}Zr_xFe_{2-2x}O_4$ (x = 0.0 to 0.6) were prepared by double sintering ceramic technique, using A.R. grade NiO, ZnO, ZrO_2 and Fe_2O_3 compounds with 99.9% purity . They were mixed in their stoichiometric proportion, milled with acetone base agate mortar for about three hours to get fine powder. The presintering was carried out at 500˚C for 24 hours in the furnace; samples were allowed to cool by natural process. These sintered powders were then pressed into pellets of desired thickness with the help of hydraulic press by applying a

pressure of 6 tones for 10 minutes on each pellet. Further these pellets were finally sintered at 1100˚C for 24 hours, cooled by natural process. The phase purity of the samples was analyzed by using X-ray diffraction method with Cu-Kα radiation. The d.c. electrical resistivity of all the samples were measured with the help of two probe method in the temperature range 400°K to 800°K. The dielectric properties of Zirconium doped Ni-Zn ferrites were measured at constant frequency 1 KHz by varying temperature with the use of LCR-Q meter.

Result and Discussion

1. X-Ray analysis

The X-ray patterns of $Ni_{0.7+x}Zn_{0.3}Zr_xFe_{2-2x}O_4$ for the typical samples are shown in fig.1. When monochromatic beam of X-ray is incident on powder sample, it is reflected, the reflected rays interfere and interference is constructive only if the path difference between the interfacing rays is in integral multiple of the wavelength of incident X-ray beam. The condition of constructive interference is given by Bragg's law,

$n\lambda = 2d\sin\theta$---------- (1)

The unit cell dimensions are determined from the d-spacing of a line by making of the cubic formula for inter-planer spacing.

$a = d\,(h^2+k^2+l^2)^{1/2}$ -------- (2)

where a – is the lattice constant.
d- is the inter-planer spacing and
(hkl)- is the miller indices.

The X-ray density dx was calculated using the following relation [8]

$$d_x = \frac{ZM}{NV} \qquad \text{--------(3)}$$

where , Z is the number of molecule per unit cell. For cubic ferrite Z = 8,
M- is molecular weight ,
N-is Avogadro's No. ($6.022 * 10^{23}$)
V – is volume of unit cell.

From XRD pattern it is confirmed that, the Ni-Zn ferrite samples have the single phase cubic spinel structure, it is formed as all the peaks in the pattern match well with the characteristic reflections of Ni-Zn ferrite reported earlier by Anil Kumar et.al. [9]. The remaining samples of the same series also show cubic spinel structure. From the XRD patterns, the lattice parameter and X-ray density of
$Ni_{0.7+x}Zn_{0.3}\ Zr_xFe_{2-2x}O_4$ system has been determined. According to ionic radii r_{Zr4+}=0.80Å, r_{Ni2+}= 0.78Å and r_{Fe3+}= 0.67Å the lattice parameter is expected to increase with increasing Zr-concentration. However, the attraction force of the oxygen ions for the tetravalent ions (Zr^{4+}) is larger than those for divalent (Ni^{2+}) and trivalent (Fe^{3+}) ions. Thus the lattice parameter must decreases linearly with increase in composition (x) and the distance between Oxygen ions and Zirconium ions is decreases , hence the bond lengths also decreases so that lattice parameter decreases .Similar result is reported by A.A.Sattar and H.M.EI-Sayed in Zr^{4+} substituted Li-Zn ferrite.

2. D.C. Resistivity

D.C. resistivity of all samples was measured by two probe method. The measurement were taken in the temperature range
400-823˚K the relationship between resistivity and temperature is given by Arrhenius as

$\rho = \rho_0 \exp(-Eg / kT)$----------(4)

Fig.2 shows logρ verses reciprocal of temperature for x = 0.1,0.3 and 0.5. This nature of electrical conductivity linearly attributed to the hopping of electron between Fe^{2+} and Fe^{3+} ions at octahedral site. The line of each sample is broken at certain temperature which is found to be in agreement with the corresponding Curie temperature. From table 2 it is observed that the activation energy in paramagnetic region (E_P) is grater than ferrimagnetic region(E_F).Activation energy going on decreasing with increase in Zr^{4+}-concentration. Curie temperature decrease with increase in Zr^{4+} content.

3. Dielectric properties

The variations of the of ε′, ε″ and tanδ with temperature at1 KHz are shown in

Fig. 3(a, b and c), respectively. The dielectric properties are measured in the temperature range of 300-800˚K at high frequency (1 KHz). The calculations are partly based on the frequency dependent measured .From these figures both ε′ and ε″ increases with increasing temperature. Similar results are obtained for different materials [10, 11 and 12]. Especially, ε′ the was found to change linearly (Fig. 3a) with the temperature intervals 300-800˚K .The rate of increase, as the temperature causes a loosening of the rigid structure, was resulted from an increase in dipole orientation and hence an increase in ε′. The variation of tanδ increases with increase in temperature. Our results are good agreement with well-known ferrites [13,14]. It may be due to space charge polarization caused by impurities or interstitials in the materials. Moreover, in narrow band semiconductors, the charge carriers are not free to move but are trapped, causing a polarization. On increasing temperature, the number of charge carriers increases exponentially and thus produces further space charge polarization and hence leads to a rapid increase in the dielectric constant. Of course, both types of charge carriers n-type and p-type contribute to the polarization. However, the p-type contribution is negligible where the dominant charge carriers are holes as showed previously [18, 19]. It is clear that the conductivity increases with increasing temperature. Similar results have been reported in literature [15–20], suggesting that the process of dielectric polarization takes place through a mechanism similar to the conduction process. The increase in the electrical conductivity at low temperature is attributed to the impurities, which reside at the grain boundaries [21]. These impurities lie below the bottom of the conduction band and thus it has small activation energy. This means that the contribution to the conduction mechanism comes from the grain boundaries while it mainly results from the grains for higher temperature.

Acknowledgement

The authors are thankful to Central Instruments Laboratory, University of Hyderabad for providing the XRD data. The authors are also thankful to Prof.M.V.N. Ambika Prasad (Department of Materials Science, Gulbarga University.) for his fruitful discussion.

References

[1] M. Sugimoto, J.Am.Soc. 82(2) (1999) 269.
[2] Enlc Zhou ,Shifeng Yan. J. Magn. Magn. Mater. 292 (2005)304-309.
[3] O.F. Caltun et.al. J. Magn. Magn. Mater.242-245 (2002) 160.
[4] R.V. Mangalraja. Et.al. J. Magn. Magn. Mater.253 (2002) 56-64.
[5] M.Guyot, J. Magn. Magn. Mater.18(1990) 925.
[6] A.M.Abdeen , J. Magn. Magn. Mater.192(1999).
[7] G.Ranga Mohan D.Ravinder et.al., Materials Letters 40(1999) 39-45.
[8] K.J.Standley “Oxide magnetic material” Clarendon press Oxford (1962).
[9] P.S. Anil Kumar, Mater.Lett.27 (1996)293.
[10] A. Tataroglu, S. Altındal, M.M. Bulbul, Microelectron. Eng. 81(2005) 140.
[11] R.D. Gould, S.A. Awan, Thin Solid Films 469 (2003) 184.
[12] T. Ozaki, T. Ogasawara, T. Kosugi, T. Kamada, Physica B 263(1999) 333.
[13] M.M. Bulbul, Microelectronic Engineering 84 (2007) 124–128.
[14] A. Verma, O.P. Thakur, C. Prakash, T.C. Goel, R.G. Mendiratta Mate. Sci. Eng. B 116 (2005) 1–6.
[15] R.D. Gould, Thin Solid Films 423 (2003) 267.
[16] K. Prabakar, S.K. Narayandass, D. Mangalaraj, Phys. Stat. Sol. 199 (3) (2003) 507.
[17] A.A. Sattar, S.A. Rahman, Phys. Stat. Sol. (a) 200 (2) (2003) 415.

[18] C. Fanggao, G.A. Saunders, E.F. Lambson, R.N. Hampton, J. Appl. Poly. Sci. 34 (1996) 425.
[19] C. Ye, Z. Ning, M. Shen, S. Cheng, Z. Gan, J. Appl. Phys 83 (11)(1998) 5978.
[20] R.D. Gould, S.A. Awan, Thin Solid Films 433 (2003) 309.
[21] M.S. Mattsson, G.A. Niklasson, K. Forsgren, A. Harsta, J. Appl.Phys. 85 (4) (1999) 2185.

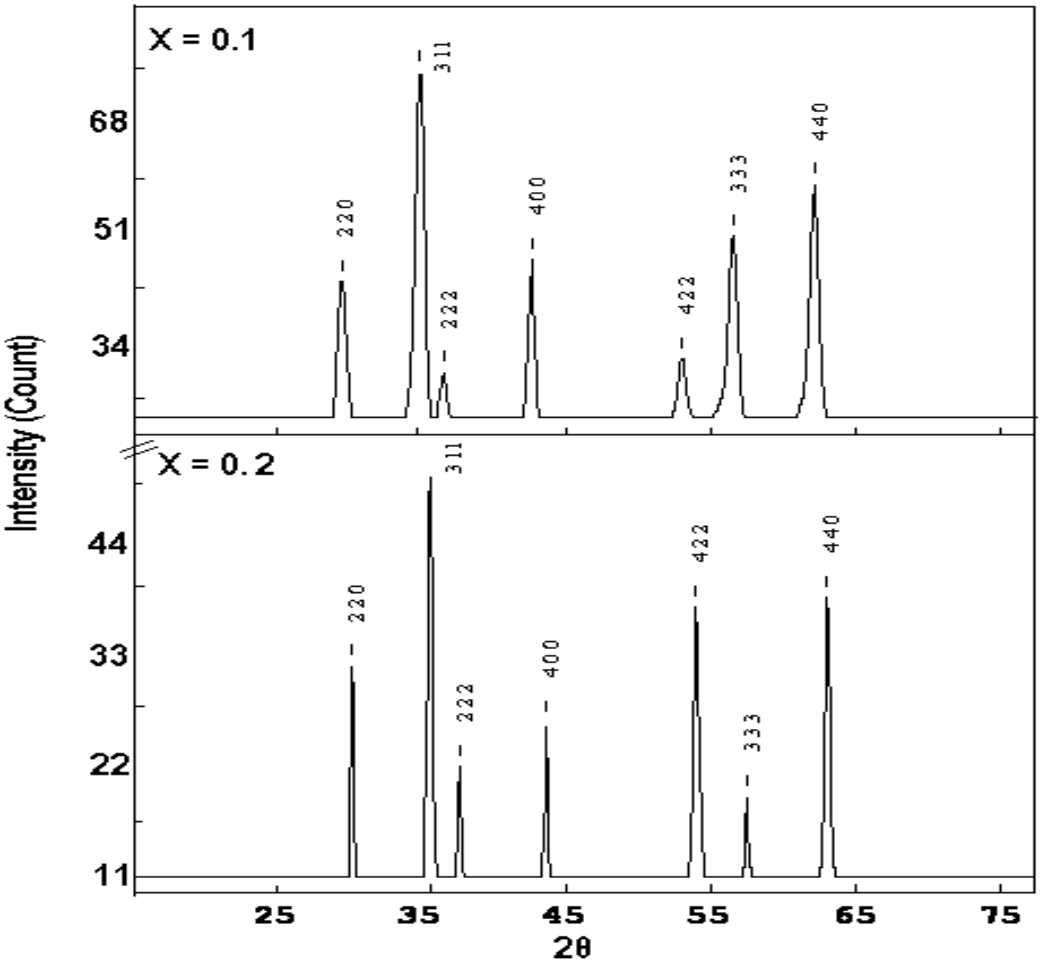

Fig. 1- X-Ray pattern for $Ni_{0.7+x}Zn_{0.3}Zr_xFe_{2-2x}O_4$ system.

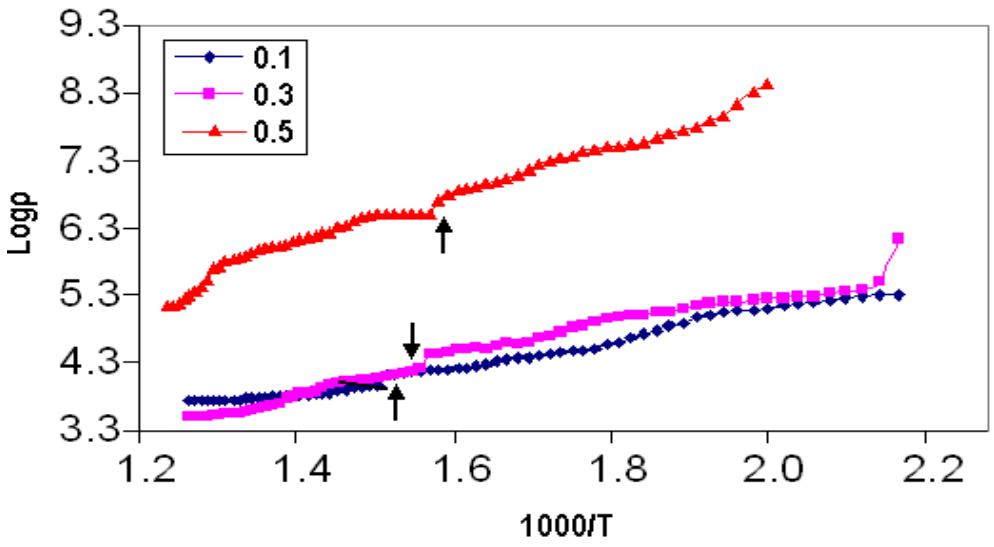

Fig. 2- Plots of Logρ verses $10^3/T$ for $Ni_{0.7+x}Zn_{0.3}Zr_xFe_{2-2x}O_4$ system.

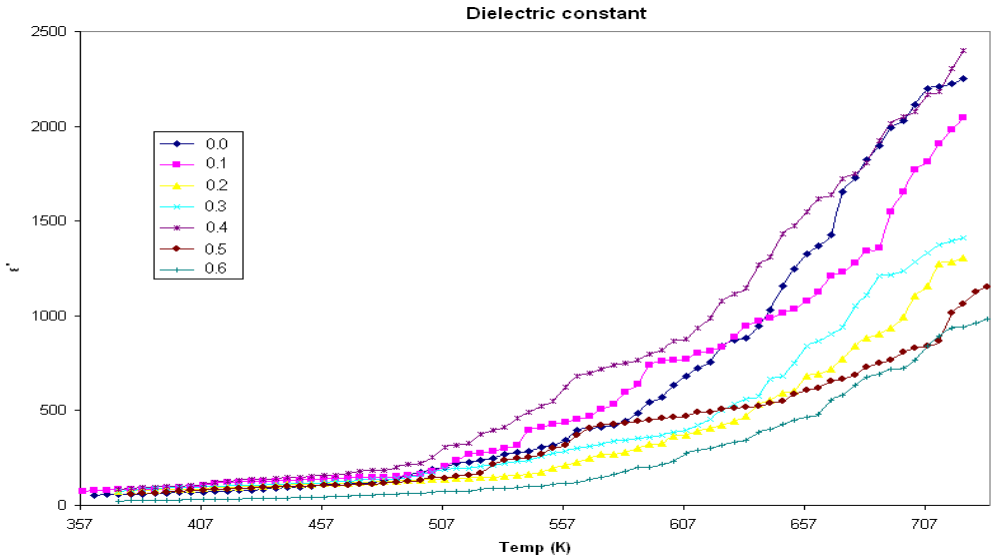

Fig. 3a- Variation of dielectric constant with temperature.

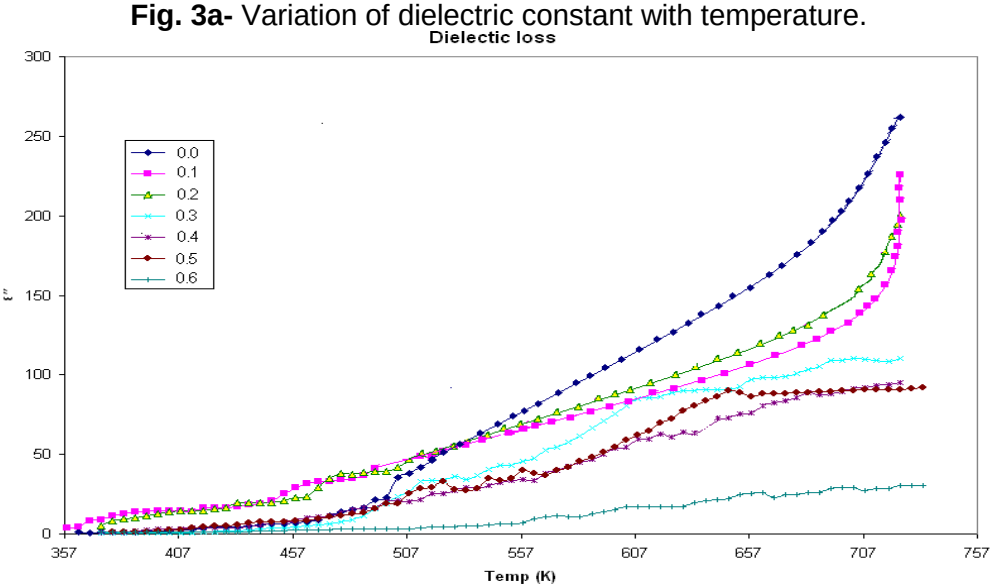

Fig. 3b- Variation of dielectric loss with temperature.

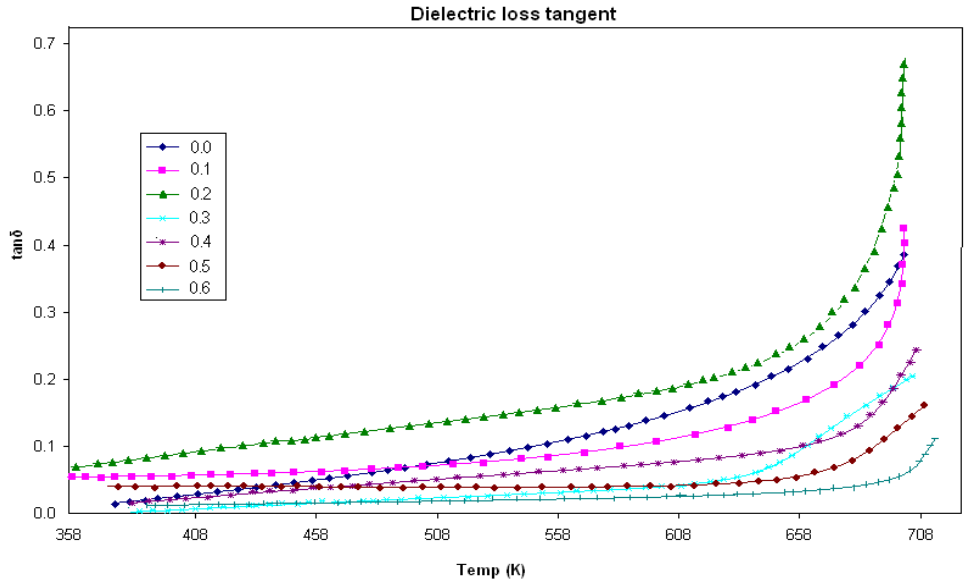

Fig. 3c- Variation of dielectric loss tangent with temperature.

Table 1- Lattice constant (a), X-ray density (dx), Bulk density (d) and porosity (p) for $Ni_{0.7+x}Zn_{0.3}Zr_xFe_{2-2x}O_4$ system.

Composition	Lattice constant (Å)	X-Ray density gm/cm^3	Bulk density gm/cm^3	Porosity (%)
$Ni_{0.7}Zn_{0.3}Fe_2O_4$	8.3777	5.399	3.3350	38.24
$Ni_{0.8}Zn_{0.3}Zr_{0.1}Fe_{1.8}O_4$	8.3665	5.4463	4.7070	13.58
$Ni_{0.9}Zn_{0.3}Zr_{0.2}Fe_{1.6}O_4$	8.3540	5.557	3.2583	41.37
$Ni_{1.0}Zn_{0.3}Zr_{0.3}Fe_{1.4}O_4$	8.3248	5.7044	4.8146	15.60
$Ni_{1.1}Zn_{0.3}Zr_{0.4}Fe_{1.2}O_4$	8.3127	5.8177	3.7453	35.63
$Ni_{1.2}Zn_{0.3}Zr_{0.5}Fe_1O_4$	8.3093	5.9133	4.7533	19.62
$Ni_{1.3}Zn_{0.3}Zr_{0.6}Fe_{0.8}O_4$	8.2943	6.0344	4.3842	27.35

Table 2- Curie temperature and activation energy from d.c. plots for $Ni_{0.7+x}Zn_{0.3}Zr_xFe_{2-2x}O_4$ system.

Comp. x	Curie temp T_c (^{0}C)	Ep (eV)	E_f (eV)	Activation (ΔE) (eV)
0.0	415	0.8051	0.5994	0.2057
0.1	410	0.2883	0.1760	0.1123
0.2	420	0.3673	0.2708	0.0927
0.3	393	0.591	0.5002	0.0908
0.4	384	0.4063	0.3272	0.0791
0.5	380	0.8218	0.8175	0.0712
0.6	370	0.6686	0.6014	0.0672